2019 IEEE International Ultrasonics Symposium (IUS)
Glasgow, Scotland, October 6-9, 2019

Towards an Inverse Characterization of Third Order Elastic Constants Using Guided Waves

Michael Ponschab*, Daniel A. Kiefer, Stefan J. Rupitsch
Friedrich-Alexander-University Erlangen-Nürnberg (FAU), Sensor Technology, Erlangen, Germany
*michael.ponschab@fau.de

***Abstract*—The acoustoelastic effect describes the change in propagation velocities of elastic waves due to mechanical prestress and is based on geometric and material nonlinearity. Models describing the effect heavily depend on the knowledge of the third order elastic constants (TOEC). Established acquisition methods of these constants rely on the measurement of bulk speeds of sound and analytic calculations. In this contribution, we propose an alternative method by making use of the dispersive character of guided waves in plates. Uniaxial tensile stress is applied to homogeneous metallic plates. The changes in wavenumber are calculated from laser vibrometer aided measurements. These changes depend on a trigonometric function of the direction of wave propagation and increase linearly with the prestress amplitude. Using this prior knowledge, we perform an inverse characterization of the TOEC by iteratively fitting a numerical model of the prestressed waveguide to constants of the trigonometric relation. The proposed method is verified using simulated reference data.**

***Index Terms*—material characterization, acoustoelasticity, Lamb wave, nonlinear acoustics, inverse method**

I. Introduction

The detection of defects and cracks in plate-like structures and pipes by means of ultrasonic guided waves has become a well studied field of nondestructive testing [1], [2]. Beside defects, temperature and other environmental influences, guided waves are also sensitive to applied or residual stresses. This nonlinear behavior is described by the acoustoelastic theory [3]. The acoustoelastic effect (AEE) refers to a change in wavespeed due to large constant initial stresses. The AEE on guided waves has been used for the measurement of tensile stresses [4]–[7] and bending [8] of plates and cylinders as well as pressurized pipes [9]. Furthermore, guided waves have been applied to monitor stresses in strands [10]–[12].

A well written derivation of the acoustoelastic theory by Pao et al. can found in [3]. With the help of this bulk wave theory Gandhi et al. modeled the AEE on plane waveguides [13] and calculated the dispersive wavespeeds for biaxial tensile stresses. They applied a partial wave technique to solve the cumbersome waveguide problem. Recent improvements in solving elastodynamic waveguide problems numerically with a semi-analytical finite element method [14] or the spectral collocation method [15] accelerated the calculation of dispersion curves. Stress gradients can also be modelled well with this techniques [15], [16].

The AEE depends on both geometric and material nonlinearities. The later are taken into account in the form of higher order terms in the stress-strain relation, which depend on the third order elastic constants (TOEC). In the linear case, an isotropic medium is characterized by its density and two second order elastic constants, e.g. the Lamé parameters. If the quadratic terms are considered, three additional parameters, e.g., the Murnaghan constants, will be necessary. Modelling the stressed waveguide heavily depends on the knowledge of these higher order material constants, but unfortunatelly not for all materials reliable constants are available in the literature. The state of the art method for the determination of the third order parameters is based on ultrasonic time-of-flight measurements with both longitudinal and shear wave high frequency ultrasonic transducers under different orientations to the loading direction [17]. The small wavespeed changes require careful measurements while keeping constant laboratory conditions. For this reason, the reported material constants often exhibit great uncertainties. Muir recently suggested a one-sided approach using reflected bulk waves in plates, which basically relies on the same principle of calculating the constants analytically from a set of measurements [18].

The mentioned methods require blockshaped test specimen or thick plates and base on a set of different measurement setups to calculate the constants directly. Inverse methods gained interest for material characterization in the last years. The idea is to fit a model to measured data by iteratively adjusting the searched parameters [19]. At cost of higher computational efford, the parameters can be obtained with better precision, relying on more diverse measurement data. For example, inverse methods have been exploited to calculate linear elastic constants like Young's modulus of isotropic plates [20], [21] or the constants of orthotropic plates [22]. Resently, we proposed a method to determine the bulk wavespeeds and thickness of plates simultaneous [23]. In this contribution, we present succeeding work aiming to acquire the isotropic TOEC of thin metal plates by means of inverse methods. To the knowledge of the authors, no work has been published on this topic yet.

The contribution is organized as follows. The acquisition of stress dependent dispersion data is described in Section II. The approach to inversely characterize the TOEC is outlined in Section III. Simulation results are shown in in Section IV demonstrating the efficiency of the proposed method. Lastly, a conclusion is given in Section V.

II. Acquisition of Stress Dependent Wavenumbers

We used the measurement setup shown in Fig. 1 to obtain frequency resolved wavenumbers from space and time depen-

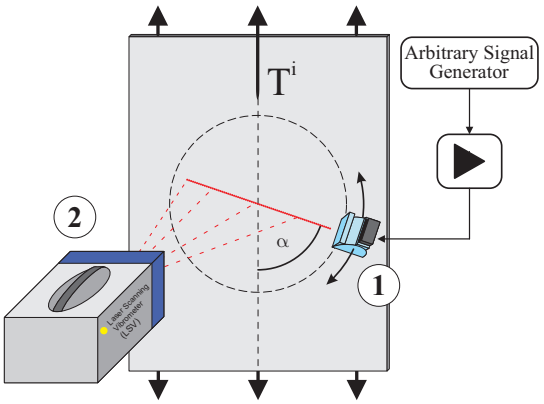

Fig. 1. Sketch of the measurement setup containing an angle beam ultrasonic transducer (1) and a laser scanning vibrometer (2). The plate is stretched uniaxially by the prestress T^{i}. The wedge transducer is stepwise rotated by angle α to the direction of stress.

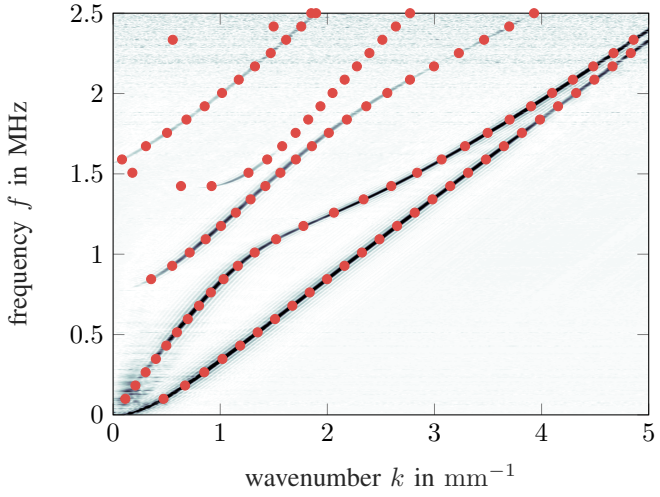

Fig. 2. Dispersion curves acquired by applying a 2D-FFT to measurement data of an aluminum plate with 2 mm thickness. The orange dots show the model output with fitted linear isotropic constants and thickness.

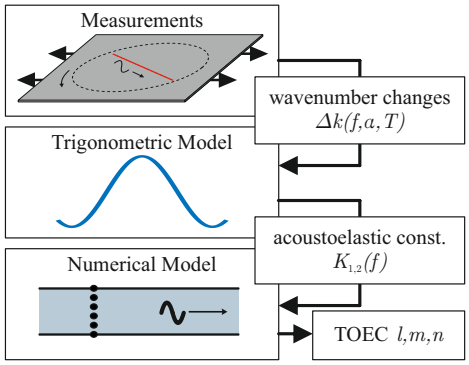

Fig. 3. Flow chart outlining the proposed procedure for the inverse characterization of TOEC.

dent Lamb wave data. We excited the zero and first order Lamb modes utilizing a variable angle beam ultrasonic transducer at different incident angles. Modes with the full transducer frequency range were excited utilizing coded signals, which provide a better signal to noise ratio due to their greater time-frequency-product [23]. The signal was generated by an arbitrary function generator.

The ultrasonic transducer was mounted on homogeneous metal plates of thicknesses $0.5\,\mathrm{mm}$ to $3\,\mathrm{mm}$. The plate was vertically clamped in a tensile testing machine, which preloaded the plate with stresses $0 \leq T^{\mathrm{i}} \leq 25\,\mathrm{MPa}$. In order to change the angle α between the preload and propagation direction, the position of the transducer was changed in discrete steps of $15°$. We measured the time dependent normal surface velocities of propagating Lamb waves using a laser scanning vibrometer (*Polytec PSV-500*). The waves were sampled at about 400 measurement points with intervals of $0.35\,\mathrm{mm}$ along a line parallel to the Lamb wave propagation direction. The time signals were sampled at a rate of $12.5\,\mathrm{MHz}$ over $200\,\mu\mathrm{s}$ and averaged one hundred times.

After preprocessing the time and space resolved data and taking the two-dimensional Fourier Transform, we obtain distinct dispersion data of propagating Lamb modes in the frequency-wavenumber-domain, which is depicted in Fig. 2 shaded in black. By applying a simple peak finding algorithm, we extract the corresponding dispersion curves with wavenumbers k_{m}.

III. Inverse Characterization of Third Order Elastic Constants

Optimizing a numerical model in order to fit data obtained by measurements is a convenient way to tune uncertain model parameters. The basic idea is to iteratively adjust the parameters $\boldsymbol{p}$ in a way that the difference between model and test data is minimized. Mathematically, this represents an inversion of a direct problem $M\colon \boldsymbol{p} \rightarrow \boldsymbol{q}$. The major difference to the classical method is the way the problem is posed. Calculating the inverse problem $M^{-1}\colon \boldsymbol{q} \rightarrow \boldsymbol{p}$ will be straight forward if an analytical model is used, which is the convenient method of acquiring the TOEC. In the presented case, we employ a numerical model, which in general results in an ill-posed problem [19]. Therefore, an iterative adjustment of the parameters $\boldsymbol{p}$ by minimization of a cost function is necessary to solve this problem. The parameters $\boldsymbol{p} = [l, m, n]$ are chosen as the TOEC defined by Murnaghan.

Fig. 3 outlines the procedure, which is described in more detail in the subsections afterwards. At first, the characterization process described in [23] is applied to the unstressed data, obtaining a basic linear plate model. Prestress dependent wavenumber changes are calculated from measurements of the prestressed plate and model data. Shi et al. [4] assumed a trigonometric dependence of the wavenumber changes on the direction of wave propagation to applied tensile stress. Two empirical so-called acoustoelastic constants (AEC) describe this relation for a single frequency and mode. We exploit this preknowledge for noise reduction by fitting the measured wavenumber changes to this relation. Finally, the unknown TOEC are inversely characterized applying a numerical model,

which calculates these AEC in dependence on the elastic constants.

A. Waveguide Model

The acoustoelastic theory, which is applied here to model a prestressed waveguide, is based on the superposition of a finite static deformation with an infinitesimal harmonic wave propagation. The theory for bulk waves gives two coordinate systems for the evaluation of the AEE, depending on the investigated setup [3]. The analysis in natural coordinates links the results to the undeformed system, also often called material coordinates. Setting up the formulas in initial coordinates, which are the coordinates of the predeformed body, refers the variables to the prestressed system. The latter concept is suitable here because the proposed measurement system is not fixed to the specimen and the measurement coordinates are not changed by deformation.

Dispersion curves of biaxially prestressed waveguides were first calculated by Gandhi et al. [13] by combining the bulk wave equations of acoustoelastic theory with the appropriate boundary conditions. Modern numerical methods solve the problem by discretizing the boundary value problem over the finite dimension of plate thickness, e.g. using spectral collocation methods [24], which results in an classical eigenvalue problem. The equations solved in our implementation may be found in [16]. The eigenvalue problem is efficiently computed in *MATLAB*, which is essential to perform an inverse characterization because the model is solved several times during each single iteration step. Calculating the dispersion curves for 1000 frequency steps and discretized with 20 points takes $5.0\,\mathrm{s}$ with an *Intel i5* CPU.

B. Characterization of Second Order Elastic Constants

In Section II the acquisition of wavenumbers k_m was described. In a first step, we characterize the second order isotropic elastic constants and the plate thickness from the extracted wavenumbers for $T^\mathrm{i} = 0$ [23]. Applying now the estimated second order constants to the linear model yields the simulated wavenumbers k_s. As Fig. 2 shows, the red dots, which refer to k_s, fit well to the measured dispersion curves. The changes in wavenumber Δk, to which the further characterization procedure refers, are calculated as the difference $\Delta k = k_\mathrm{m} - k_\mathrm{s}$. The data obtained from the measurements results in frequency f, mode m, absolute applied stress T^i and propagation angle α dependend data. The temperature is assumed to be constant.

The wavenumber changes due to initial stress are expected to be very small. Therefore, acquiring the wavenumbers with low noise is crucial for the characterization of nonlinear constants. We analyzed the measurements of plates of different material and thicknesses in order to receive a statement about expectable noise. It is supposed that Δk of an unstressed plate only depends on noise. On average of all measurements, the observed standard deviation of Δk was $\sigma = 30.8\,\mathrm{m}^{-1}$, but the best attempt reached a minimum of $\sigma = 2.0\,\mathrm{m}^{-1}$.

C. Estimation of the Acoustoelastic Constants

A characterization of the TOEC would already be possible by fitting the nonlinear model to the whole dataset described in the last subsection. Our refined approach exploits the trigonometric relation

$$\Delta k = T^\mathrm{i}\left(K_1 \cos^2(\alpha) + K_2 \sin^2(\alpha)\right). \tag{1}$$

Thereby, the wavenumber changes depend on the applied stress and the propagation angle. Shi et al. [4] proposed this model in a similar form, introducing so-called *acoustoelastic constants* (AEC) K_1, K_2, which are obtained by fitting the model function (1) to the wavenumber changes. These constants are not only functions of frequency and mode but also of second- and third order elastic constants and plate thickness. A comparision of simulated Δk for different stress configurations and fitted sinusoidal model is presented in Fig. 4 and shows that the analytic model is a good approximation to describe the wavenumber changes. Slight discrepancies arise for increasing prestress amplitudes.

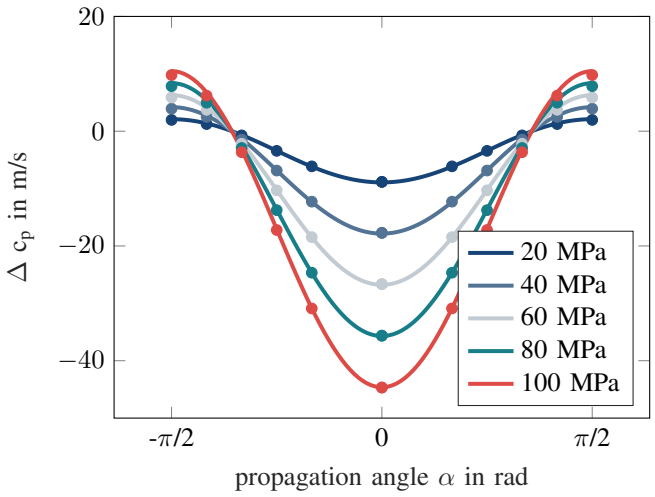

Fig. 4. Angular dependence of the change of phase velocity Δc_p due to a tensile prestress T^i of different amplitudes at angle α to guided wave propagation direction. The trigonometric relation (solid lines) is fitted to numerical model data (•).

Fitting the measured wavenumber changes to the model function (1) features two advantages:

1) The computational effort to solve the full prestressed numerical model outlined in Subsection III-A is significantly reduced. Instead of calculating the guided wave spectrum for all configurations of prestress, it is fully sufficient to calculate the AEC from two single configurations, namely

$$K_1 = \left.\frac{\Delta k}{T^\mathrm{i}}\right|_{\alpha=0} \qquad K_2 = \left.\frac{\Delta k}{T^\mathrm{i}}\right|_{\alpha=\pi/2}. \tag{2}$$

2) Exploiting the additional preknowledge how configurations of prestress influence the wavenumbers reduces the noise of measurement data. Investigations revealed, that

by fitting more data on different values of α and T^{i} to the model (1), the standard deviations can be halfed [4].

At this point, a pair of AEC for every sampled frequency and mode has been calculated. As all of these AEC depend on the same searched parameters, they build a valid basis for characterizing the TOEC.

D. Characterization of Third Order Constants

The numerical model is capable of calculating the wavenumber changes Δk of any stress configuration. In using the relation (2), the AEC K_1, K_2 are obtained by calculating the wavenumber changes for a single prestress amplitude and two angles $\alpha = \{0, \pi/2\}$. The second and third order constants as well as the initial stress tensor are kept constant. The AEC are calculated for a range of frequencies and the four lowest order modes. The corresponding phase velocity changes for a aluminium 6061 plate of $2\,\mathrm{mm}$ thickness are shown in Fig. 5. The material data is taken from [13].

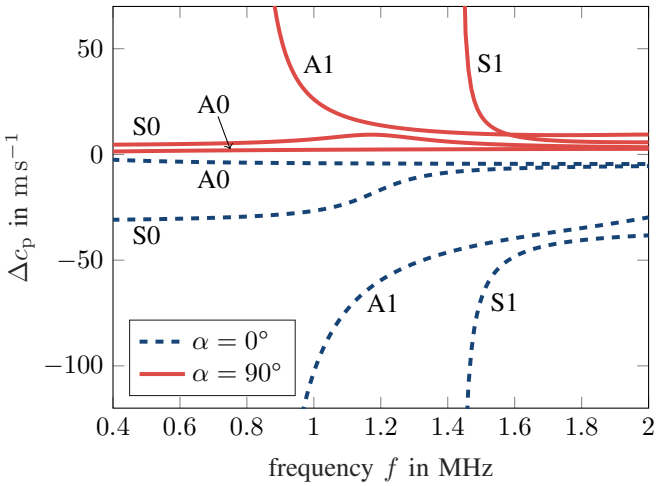

Fig. 5. Changes in phase velocity of an aluminium 6061 plate of $2\,\mathrm{mm}$ thickness for $T^{\mathrm{i}} = 80\,\mathrm{MPa}$ and $\alpha = \{0, \pi/2\}$.

Fig. 5 shows that a prestress parallel to the propagation direction decreases the phase velocity, while a prestress perpendicular to the propagation direction results in a slight increase. Like the phase velocity themselves, the changes are also strongly dispersive. This feature is exploited in the characterization process. The simulated and measured quantities $\boldsymbol{q} = [K_1^m(f), K_2^m(f)]$ with $m = \{\mathrm{S0}, \mathrm{S1}, \mathrm{A0}, \mathrm{A1}\}$, which are compared during the inverse characterization, consist of the frequency dependent AEC for each mode. An example for q is shown in Fig. 6. The vertical solid line separates data related to K_1 and K_2, while the dashed lines separate the modes. Each mode contains frequency dependent data points for the frequency range of $0.5 - 2\,\mathrm{MHz}$.

IV. Results

The proposed measurement procedure consists of a number of time consuming single measurement steps. So far, we were not able to keep all environmental influences, e.g. temperature, constant during the measurement time of several hours. Consequently, reliable measurement data can be not presented at this point and the results shown here rely on simulated data only. A reconsideration of the measurement setup in future work may speed up the process and get rid of this systematic errors.

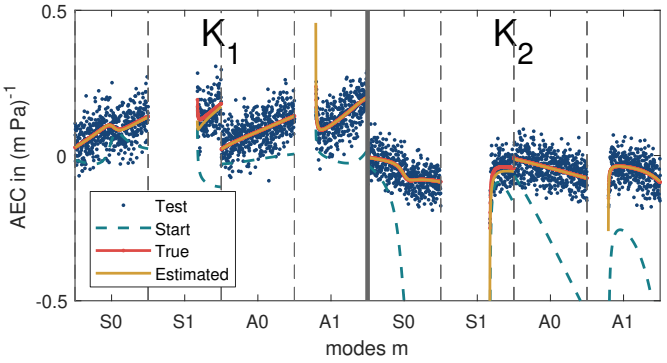

Fig. 6. AEC K_1 (left) and K_2 (right) for the four lowest order modes, separated by vertical dashed lines. The data for each mode corresponds to a frequency range of $0.5 - 2\,\mathrm{MHz}$. Each line corresponds to another set of TOEC: start parameters prior to characterization (dashed green), estimated parameters after characterization (solid yellow) and targeted true parameters (solid red), related to the noisy test data (blue dots).

In order to verify the proposed method, we used a set of simulated data to which we added noise with a standard deviation $\sigma = 30.8\,\mathrm{m^{-1}}$, observed during measurements (see Section III-B). With the material constants from [13] a test dataset was calculated, which follows the considered measurement setup and contains wavenumber changes of the four lowest order modes, sampled at 500 frequency steps for four amplitudes of applied stress and six angles to the propagation direction. The blue dots in Fig. 6 refer to the retrieved AEC from the test data. The red lines present the true data without noise. Altering the start parameters may lead to totally different dispersion curves. An example is given as dashed green lines. Even under this noisy conditions, the algorithm converges to matching TOEC, represented by yellow lines.

For further verification, we performed Monte Carlo simulations consisting of 130 single estimations with different start parameters. Since no prior knowledge about the true TOEC will be available in most cases, we altered the start parameters randomly in the range of $\pm 100\,\%$. The inverse method converged in $85.9\,\%$ cases. The residual deviation of estimated parameters compared to the true ones was below $1\,\%$ for the constants m, n, but $3.6\,\%$ for the constant l. This indicates that the test data is less sensitive to l and other setups, e.g., considering SH-modes, might be necessary to reduce the uncertaincy.

V. Conclusion

This contribution outlined the development of a guided wave based determination of isotropic third order elastic constants. Laser vibrometry aided measurements of waveguide modes and a numerical model are used to inversely characterize the

higher order material constants. Unfortunatelly, appropriate measurement data could not be provided at this moment, but verfications were conducted with realistic simulation data. The results demonstrate that the proposed method might be a promissing alternative to the established methods of acquiring the non-linear constants and is especially useful in cases where platelike test specimen should be investigated.

The main problem, leading to a failure of the measurements, was the long measurement time of several hours and a lot of necessary manual adjustments arising from the chosen setup. The environmental conditions, especially the temperature, could not be held constant over that time. Further work may concentrate alternative setups for example by using a permanently attached piezoeelectric disc for excitation and a spider web like placement of measurement pionts. Besides temperature, small anisotropy effects, e.g., originating from rolling of the metal plates during production may influence the acquired wavenumbers and should be taken into account in future work.

ACKNOWLEDGMENT

The Chair of Sensor Technology is grateful for the financial support by Diehl Metering.

REFERENCES

[1] V. Giurgiutiu, *Structural health monitoring with piezoelectric wafer active sensors*. Amsterdam: Academic Press/Elsevier, 2008.

[2] T. Clarke, P. Cawley, P. D. Wilcox, and A. J. Croxford, "Evaluation of the damage detection capability of a sparse-array guided-wave SHM system applied to a complex structure under varying thermal conditions," *IEEE Transactions on Ultrasonics, Ferroelectrics, and Frequency Control*, vol. 56, no. 12, pp. 2666–2678, 2009.

[3] Y. H. Pao, W. Sachse, and H. Fukuoka, "Acousto-elasticity and Ultrasonic Measurement of Residual Stresses," *Physical Acoustics*, no. XVII, pp. 61–142, 1984.

[4] F. Shi, J. E. Michaels, and S. J. Lee, "In situ estimation of applied biaxial loads with Lamb waves," *The Journal of the Acoustical Society of America*, vol. 133, no. 2, p. 677, 2013.

[5] S. Roy, P. Ladpli, and F.-K. Chang, "Load monitoring and compensation strategies for guided-waves based structural health monitoring using piezoelectric transducers," *Journal of Sound and Vibration*, vol. 351, pp. 206–220, 2015.

[6] A. C. Kubrusly, A. Braga, N. Pérez, J. C. Adamowski, T. F. de Oliveira, and J. v. d. Weid, "Mechanical Strain Monitoring in Plates Using Wavelet Coherence Based Filter of Wideband Ultrasonic Guided Waves," *Physics Procedia*, vol. 70, pp. 393–397, 2015.

[7] J. Quiroga, L. Mujica, R. Villamizar, M. Ruiz, and J. Camacho, "PCA Based Stress Monitoring of Cylindrical Specimens Using PZTs and Guided Waves," *Sensors*, vol. 17, no. 12, p. 2788, 2017.

[12] B. Dubuc, A. Ebrahimkhanlou, and S. Salamone, "Higher order longitudinal guided wave modes in axially stressed seven-wire strands," *Ultrasonics*, vol. 84, pp. 382–391, 2018.

[8] A. Bulletti and L. Capineri, "Interdigital Piezopolymer Transducers for Time of Flight Measurements with Ultrasonic Lamb Waves on Carbon-Epoxy Composites under Pure Bending Stress," *Journal of Sensors*, vol. 2015, pp. 1–11, 2015.

[9] B. Dubuc, A. Ebrahimkhanlou, and S. Salamone, "Effect of pressurization on helical guided wave energy velocity in fluid-filled pipes," *Ultrasonics*, vol. 75, pp. 145–154, 2017.

[10] S. Chaki and G. Bourse, "Guided ultrasonic waves for non-destructive monitoring of the stress levels in prestressed steel strands," *Ultrasonics*, vol. 49, no. 2, pp. 162–171, 2009.

[11] I. Bartoli, G. Castellazzi, A. Marzani, and S. Salamone, "Prediction of stress waves propagation in progressively loaded seven wire strands," in *Sensors and Smart Structures Technologies for Civil, Mechanical, and Aerospace Systems 2012*, ser. SPIE Proceedings, M. Tomizuka, C.-B. Yun, and J. P. Lynch, Eds. SPIE, 2012, p. 834505.

[13] N. Gandhi, J. E. Michaels, and S. J. Lee, "Acoustoelastic Lamb wave propagation in biaxially stressed plates," *The Journal of the Acoustical Society of America*, vol. 132, no. 3, pp. 1284–1293, 2012.

[14] M. Mazzotti, A. Marzani, I. Bartoli, and E. Viola, "Guided waves dispersion analysis for prestressed viscoelastic waveguides by means of the SAFE method," *International Journal of Solids and Structures*, vol. 49, no. 18, pp. 2359–2372, 2012.

[15] B. Dubuc, A. Ebrahimkhanlou, and S. Salamone, "Computation of propagating and non-propagating guided modes in nonuniformly stressed plates using spectral methods," *The Journal of the Acoustical Society of America*, vol. 143, no. 6, p. 3220, 2018.

[16] M. Ponschab, D. A. Kiefer, and S. J. Rupitsch, "Berechnung der auswirkung mechanischer spannungen auf die ausbreitung von lamb-wellen," in *Fortschritte der Akustik - DAGA 2019*, vol. 2019, pp. 1156–1159.

[17] D. S. Hughes and J. L. Kelly, "Second-Order Elastic Deformation of Solids," *Physical Review*, vol. 92, no. 5, pp. 1145–1149, 1953.

[18] D. D. Muir, "One-sided ultrasonic determination of third order elastic constants using angle-beam acoustoelasticity measurements," Ph.D. dissertation, Georgia Institute of Technology, Georgia, 2019-08-01.

[19] S. J. Rupitsch, *Piezoelectric Sensors and Actuators: Fundamentals and Applications*, ser. Topics in Mining, Metallurgy and Materials Engineering. Berlin: Springer, 2019.

[20] M. Sale, P. Rizzo, and A. Marzani, "Semi-analytical formulation for the guided waves-based reconstruction of elastic moduli," *Mechanical Systems and Signal Processing*, vol. 25, no. 6, pp. 2241–2256, 2011.

[21] L. Ambrozinski, P. Packo, L. Pieczonka, T. Stepinski, T. Uhl, and W. J. Staszewski, "Identification of material properties - efficient modelling approach based on guided wave propagation and spatial multiple signal classification," *Structural Control and Health Monitoring*, vol. 22, no. 7, pp. 969–983, 2015.

[22] S. Johannesmann, J. Düchting, M. Webersen, L. Claes, and B. Henning, "An acoustic waveguide-based approach to the complete characterisation of linear elastic, orthotropic material behaviour," *tm Technisches Messen Plattform für Methoden, Systeme und Anwendungen der Messtechnik*, vol. 85, no. 7-8, pp. 478–486, 2018.

[23] M. Ponschab, D. A. Kiefer, and S. J. Rupitsch, "Simulation-Based Characterization of Mechanical Parameters and Thickness of Homogeneous Plates Using Guided Waves," *IEEE Transactions on Ultrasonics, Ferroelectrics, and Frequency Control*, 2019.

[24] B. Dubuc, A. Ebrahimkhanlou, and S. Salamone, "A spectral method for computing guided waves in stressed plates and rods," in *Health Monitoring of Structural and Biological Systems XII*, T. Kundu, Ed. SPIE, 2018, p. 70.